Decreased Fetal Size Is Associated With β-Cell Hyperfunction in Early Life and Failure With Age

Manu V. Chakravarthy,[1] Yimin Zhu,[1] Mitchell B. Wice,[1] Trey Coleman,[1] Kirk L. Pappan,[2] Connie A. Marshall,[2] Michael L. McDaniel,[2] and Clay F. Semenkovich[1,3]

OBJECTIVE—Low birth weight is associated with diabetes in adult life. Accelerated or "catch-up" postnatal growth in response to small birth size is thought to presage disease years later. Whether adult disease is caused by intrauterine β-cell–specific programming or by altered metabolism associated with catch-up growth is unknown.

RESEARCH DESIGN AND METHODS—We generated a new model of intrauterine growth restriction due to fatty acid synthase (FAS) haploinsufficiency (FAS deletion [FASDEL]). Developmental programming of diabetes in these mice was assessed from in utero to 1 year of age.

RESULTS—FASDEL mice did not manifest catch-up growth or insulin resistance. β-Cell mass and insulin secretion were strikingly increased in young FASDEL mice, but β-cell failure and diabetes occurred with age. FASDEL β-cells had altered proliferative and apoptotic responses to the common stress of a high-fat diet. This sequence appeared to be developmentally entrained because β-cell mass was increased in utero in FASDEL mice and in another model of intrauterine growth restriction caused by ectopic expression of uncoupling protein-1. Increasing intrauterine growth in FASDEL mice by supplementing caloric intake of pregnant dams normalized β-cell mass in utero.

CONCLUSIONS—Decreased intrauterine body size, independent of postnatal growth and insulin resistance, appears to regulate β-cell mass, suggesting that developing body size might represent a physiological signal that is integrated through the pancreatic β-cell to establish a template for hyperfunction in early life and β-cell failure with age. ***Diabetes*** **57:2698–2707, 2008**

Low birth weight predisposes to type 2 diabetes, cardiovascular disease, and premature death (1,2), prompting the hypothesis (3) that impairing growth in early life programs metabolic disease in adulthood. Much of this programming is attributed to postnatal catch-up growth, which is linked to insulin resistance and cardiovascular disease later in life (4). Modeling impaired growth in utero using calorie restriction (5), protein malnutrition (6), prenatal glucocorticoid administration (7), or ligation of the uterine arteries (8) produces catch-up growth and glucose intolerance. Catch-up growth is associated with changes in food intake, metabolism, and insulin resistance that confound the search for mechanisms linking low birth weight and adult disease. In particular, insulin resistance increases β-cell mass (9) and makes it difficult to determine whether adult disease is caused by in utero β-cell–specific programming instead of altered body composition and feeding behavior associated with accelerated postnatal growth.

Insulin and its downstream signals are critical for growth and development in species ranging from worms and insects to mammals (10–15). In *Drosophila*, body size is sensed in the fat body (equivalent to the vertebrate liver) to antagonize insulin-induced growth by ecdysone (16). If an analogous process occurs in mammals, β-cells are likely involved because they are affected by mediators of body size, including insulin, amino acids, and other signals (17). These factors also regulate fatty acid synthase (FAS), which catalyzes the first committed step in fatty acid biosynthesis (18). FAS is regulated by nutrients independent of insulin, suggesting that it could be important for nutrient-dependent growth. Its global loss results in early embryonic lethality (19). Tissue-specific inactivation of FAS is possible (20), and, surprisingly, the loss of FAS in pancreatic β-cells has no effect on β-cell mass or the capacity to secrete insulin (21). Thus, FAS, unlike glucokinase (22) and insulin receptor substrate (IRS)-2 (23), is not required for normal β-cell function.

Here, we report that FAS heterozygous mice are born small yet have expanded β-cell mass and increased insulin secretion without insulin resistance. This hyperplastic β-cell phenotype was reversed by promoting growth in utero, and increased β-cell mass was confirmed in another model of intrauterine growth restriction (IUGR). Despite the absence of catch-up postnatal growth, FAS-deficient mice develop diet-induced diabetes and β-cell failure with age.

RESEARCH DESIGN AND METHODS

Protocols were approved by the Washington University Animal Studies Committee. $FAS^{flox/flox}$ mice in a mixed (BL/6 and 129) background (20) were mated to $EIIaCre^{+/-}$ transgenic mice (24) to yield mice heterozygous for the floxed allele with (FAS deletion [FASDEL]) and without (wild type) Cre. Littermates were used as controls for all experiments. Confirmation of FAS gene rearrangement and genotyping were as described (20). Mice expressing uncoupling protein (UCP)-1 in skeletal muscle (UCP-Tg) (25) at low levels do not have growth restriction, but those with high-level expression (26) are runted and were used in this study. Standard chow was Purina 5053. Mice were fed a Western diet (Harlan-Teklad TD88137) for 10 weeks at various ages.

Female wild-type (wt/flox $EIIaCre^{-}$) or UCP-Tg mice were mated for 1 night (1700–0600 h) and observed for the presence of a vaginal plug. Sperm in the vaginal smear marked day 0.5 of pregnancy. Females were placed in individual maternity cages until E18.5, when fetuses were delivered by

From the [1]Department of Medicine, Division of Endocrinology, Metabolism and Lipid Research, Washington University, St. Louis, Missouri; the [2]Department of Pathology and Immunology, Washington University, St. Louis, Missouri; and the [3]Department of Cell Biology and Physiology, Washington University, St. Louis, Missouri.

Corresponding author: Clay F. Semenkovich, csemenko@wustl.edu.

Received 24 March 2008 and accepted 19 June 2008.

Published ahead of print at http://diabetes.diabetesjournals.org on 30 June 2008. DOI: 10.2337/db08-0404.

See accompanying commentary, p. 2563.

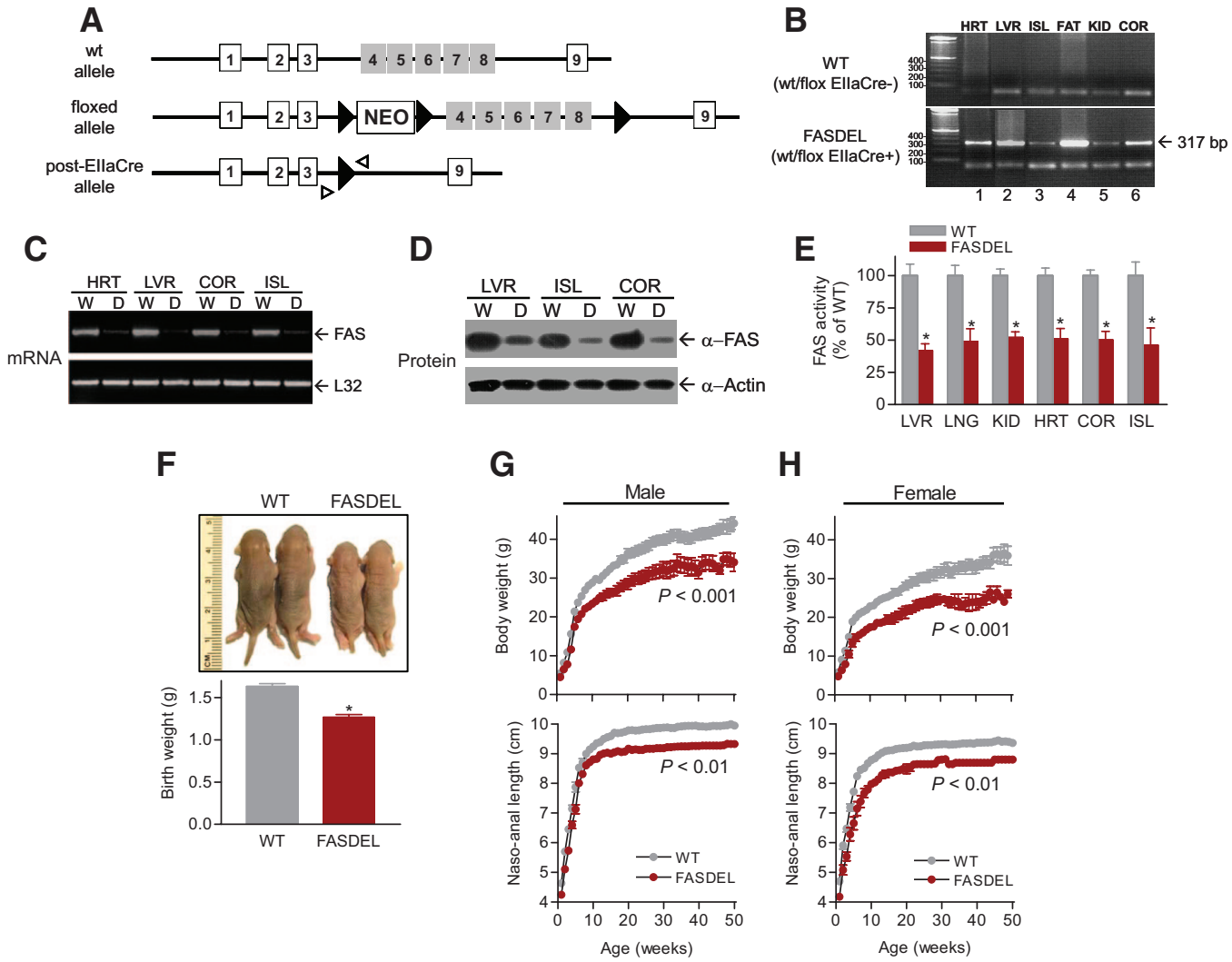

FIG. 1. Generation of FASDEL mice. *A*: FAS$^{flox/flox}$ mice with loxP sites (▶) flanking exons 4–8 (▨) were mated with EIIaCre$^{+/-}$ animals to yield FAS-deficient wt/flox EIIaCre^{+} (post-Cre allele; FASDEL) and littermate control wt/flox EIIaCre- mice (wt). *B*: DNA from heart (HRT), liver (LVR), islets (ISL), epididymal fat pads (FAT), kidney (KID), and cerebral cortex (COR) produced a 317-bp product (*lanes 1–6*, *bottom panel*) using the primers denoted by small arrowheads in *A*, indicating appropriate deletion of exons 4–8 of the *FAS* gene. This product was absent in wild-type (WT) tissues (*top panel*). *C–E*: RT-PCR for *FAS* and *L32* expression (*C*), Western blotting for FAS and actin (*D*), and FAS enzyme activity (*E*) in the indicated tissues from wild-type (WT) and FASDEL mice. *F*: Wild-type (WT) and FASDEL pups at birth (*top panel*) and their body weight (*bottom panel*). *G* and *H*: Growth curves of male (*G*) and female (*H*) wild-type (WT) and FASDEL mice depicting body weight (*top panel*) and naso-anal length (*bottom panel*) with age. *E–H*: Results are means ± SE of 12–15 animals per group. *$P < 0.05$ vs. the corresponding wild-type mice. (Please see http://dx.doi.org/10.2337/db08-0404 for a high-quality digital representation of this image.)

C-section, body weights and nasoanal lengths were recorded, and mice were analyzed.

Serum glucose, cholesterol, triglycerides, free fatty acids, C-peptide, insulin, and leptin; body composition and indirect calorimetry; glucose and insulin tolerance tests; and FAS enzyme activity from freshly harvested tissues were assayed as described (20,21). Food intake was measured over 1 week in metabolic cages, following a week of acclimatization, and expressed as a function of lean body mass ($g^{0.75}$). Feed efficiency was calculated as the ratio of body weight gained per day over the 10-week high-fat feeding period to food intake per day.

Islet isolation and insulin secretion. Pancreatic islets were isolated by collagenase digestion and hand-picked for secretion assays as described (21). Ten islets of similar size per condition were cultured in media containing either 3 or 16.7 mmol/l glucose, and insulin secreted in the media was assayed. Insulin content was measured as described (21,27).

Hyperglycemic clamp studies. A square-wave hyperglycemic clamp was performed (28). Indwelling catheters were placed into the right internal jugular veins of mice, and animals recovered for 3 days. Saline was infused by microinjector pump for 30 min then baseline insulin and C-peptide were measured. Twenty percent D-glucose was infused rapidly to achieve target glucose of 300–350 mg/dl, which was maintained for 2 h with frequent monitoring. Tail bleeds were performed every 30 min to sample serum insulin. C-peptide was assayed at the end of the clamp.

Histology, immunohistochemistry, and morphometry. E18.5 embryos were fixed in 10% buffered formalin and embedded in paraffin. Then, 10-μm sections made through the entire embryo were stained with hematoxylin and eosin. Pancreata were dissected from adults and fetuses, weighed, immersion fixed in Bouin's solution, and embedded in paraffin, and 10 separate 5-μm sections 150–200 μm apart were mounted. Immunohistochemical and morphometric analyses for islet area, architecture, β-cell density, and β-cell and non–β-cell mass by point-counting morphometry utilized described methods (21,27–29). Unless otherwise specified, images are representative of eight sections from a total of five to six animals per group.

For β-cell proliferation and apoptosis, sections were double immunostained with anti-insulin and either anti–proliferating cell nuclear antigen (PCNA) (1:200; Cell Signaling) or anticleaved caspase-3 (1:1,000; Cell Signaling) followed by appropriate secondary antibodies (Vector). At least 500–1,000 β-cell nuclei were counted per pancreas (three to four pancreata per condition), and data are expressed as the percentage of insulin plus PCNA (or cleaved caspase-3)-positive cells. Pancreatic, brain, and whole-mount embryo sections were also stained with anti–^{473}Ser-phosphorylated Akt (1:1,000; Cell Signaling) and anti-insulin (1:500; Sigma-Aldrich) then detected with appropriate reagents.

Adipose tissue from gonadal fat pads was fixed in formaldehyde, and then 10-μm sections were mounted on glass slides and stained with hematoxylin

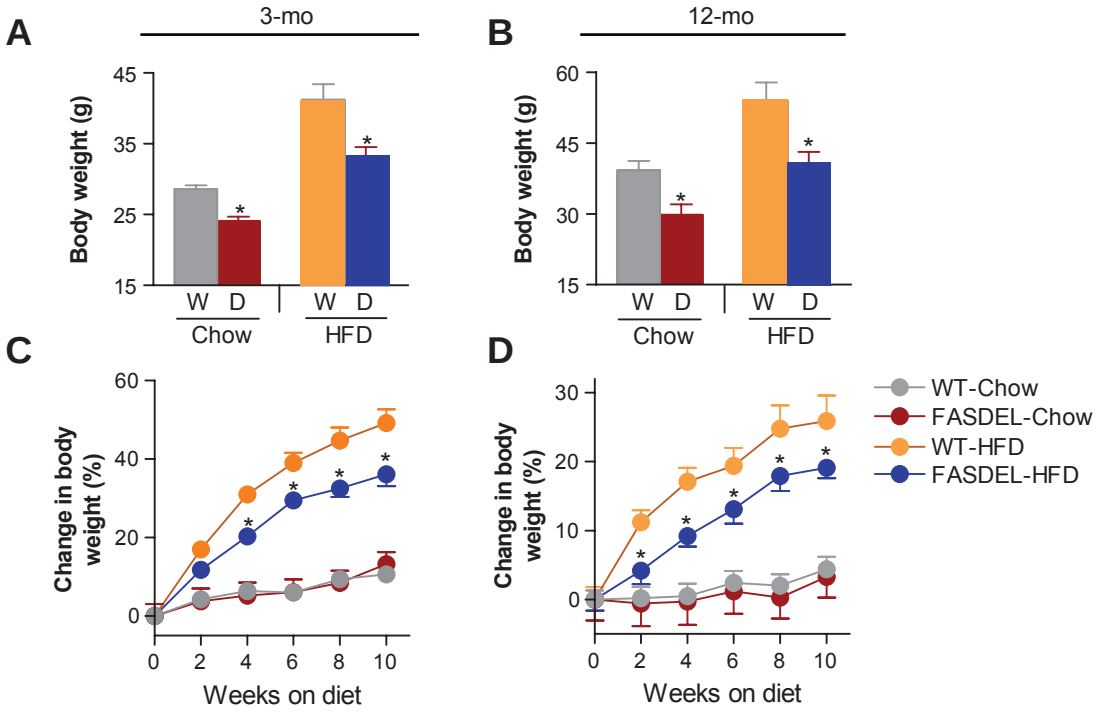

FIG. 2. Postnatal FASDEL mice do not catch up in weight despite high fat feeding. *A* and *B*: Body weight on standard chow and HFD at 3 (*A*) and 12 (*B*) months of age. D, FASDEL; W, wild type. *C* and *D*: Percent change in body weight over the 10-week HFD feeding period at 3 (*C*) and 12 (*D*) months. Results are means ± SE of 8–10 animals per group. *$P < 0.05$ vs. the corresponding wild-type mice. *C* and *D*: △, wild type/standard chow diet; ▲, FASDEL/standard chow diet; ○, wild type/HFD; ●, FASDEL/HFD.

and eosin. Diameter and area were measured in at least 300 cells per mouse in each group with MetaVue imaging software (version 6.1; Molecular Devices).

In vitro apoptosis. Apoptosis was measured in islets cultured overnight in 10 mmol/l glucose RPMI media containing 10% fetal bovine serum using the ApoPercentage kit (Biocolor), as described (29). Apoptotic cells, which appeared bright pink against the white background of phenol red–free RPMI were counted manually in a blinded fashion.

RT-PCR and immunoblotting. Snap-frozen tissue samples in liquid nitrogen were processed for RNA extraction using Trizol, cDNA was prepared by reverse transcription, and real-time PCR was performed (20,21). Primers were FAS (forward 5′-AGGCTACACAGGCTCCAAATGA-GTACC-3′, reverse 5′-AACCAACTGAACCTGAGCACACTGC-3′) and L32, an invariant control (forward 5′-TAAGCGAAACTGGCGGAAAC-3′, reverse 5′-TCATTTTCTTCGCTGC GTAGC-3′).

Tissue samples were homogenized in a buffer containing protease and phosphatase inhibitors (20). Twenty-five micrograms of each tissue protein extract was resolved on SDS-PAGE, transferred to polyvinylidene fluoride membranes, and blotted using the following antibodies: FAS (1:1,000; a generous gift from Sonia Naǰjar), total and ^{473}Ser-phosphorylated Akt (1:1,000; Cell Signaling), pancreatic duodenal homeobox factor-1 (1:1,000; Upstate), total and ^{389}Thr p70S6 kinase (1:1,000; Cell Signaling), IRS-2 (1:500; Upstate), UCP-1 (1:1,000; Alpha Diagnostics), and actin (1:5,000; Sigma-Aldrich). After incubation with the appropriate secondary antibodies (1:7,500), bands were detected by chemiluminescence (ECL kit; Amersham) (20).

Statistics. Values are expressed as means ± SE. Statistical comparisons were performed using an unpaired, two-tailed Student's *t* test (when two groups were analyzed) or ANOVA. If the overall *F* was found to be significant for the latter, comparisons between means were made using appropriate post hoc tests. Correlations between birth weight (independent variable) and β-cell mass (dependent variable) were studied using linear regression models. *P* values ≤0.05 were considered significant.

RESULTS

FAS heterozygous mice are haploinsufficient. We generated mice with whole-body heterozygous FASDEL by crossing FAS$^{flox/flox}$ mice (20) with EIIaCre$^{+/-}$ transgenic mice (24), which delete loxP-flanked DNA at the two- to eight-cell stage. FASDEL (FAS wt/flox EIIaCre^{+}) mice had exons 4–8 deleted (Fig. 1*A*). FAS gene rearrangement was demonstrated by Southern blotting and by PCR (20,21) in an assay yielding a 317-bp product (Fig. 1*B*, *bottom*). FAS message, protein, and enzyme activity were decreased by ~50% in FASDEL tissues (Fig. 1*C–E*). There were no genotype differences in placental weights or morphology (not shown).

FASDEL mice were haploinsufficient. FAS$^{flox/flox}$ × EIIaCre$^{+/-}$ crosses yielded a 3:1 ratio of wild-type to FASDEL pups (1:1 predicted). There was no sex difference with this cross, but female FASDEL mice mated to wild-type males produced fewer surviving heterozygous pups than the reciprocal cross. To minimize the effects of maternal environment and increase FASDEL yield, pregnancies were carried by wt/flox EIIaCre^{-} (wild-type) females.

FAS haploinsufficiency was manifested by a 22% decrease in birth weight (Fig. 1*F*) and a persistent decrease in weight and length without catch-up growth (Fig. 1*G* and *H*). EIIaCre mice (without flox) studied in parallel grew normally, indicating that the phenotype was not mediated by Cre. Postnatal survival in FASDEL pups was normal. FASDEL mice suckled appropriately and remained runted postweaning, despite normal food intake and oxygen consumption (online appendix Table 1 [available at http://dx.doi.org/10.2337/db08-0404]).

Early growth restriction impairs β-cell reserve with age. Chow-fed, 3-month-old FASDEL mice had lower serum glucose compared with wild-type mice. Insulin content of whole pancreas and isolated islets was increased (online appendix Table 1). Free fatty acids were decreased by ~30% in 3-month-old FASDEL mice, suggesting relative hyperinsulinemia (since insulin suppresses lipolysis). In contrast, chow-fed, 12-month-old FASDEL mice tended to have higher fasting glucose, hypoinsulinemia, and decreased whole-pancreas and islet insulin con-

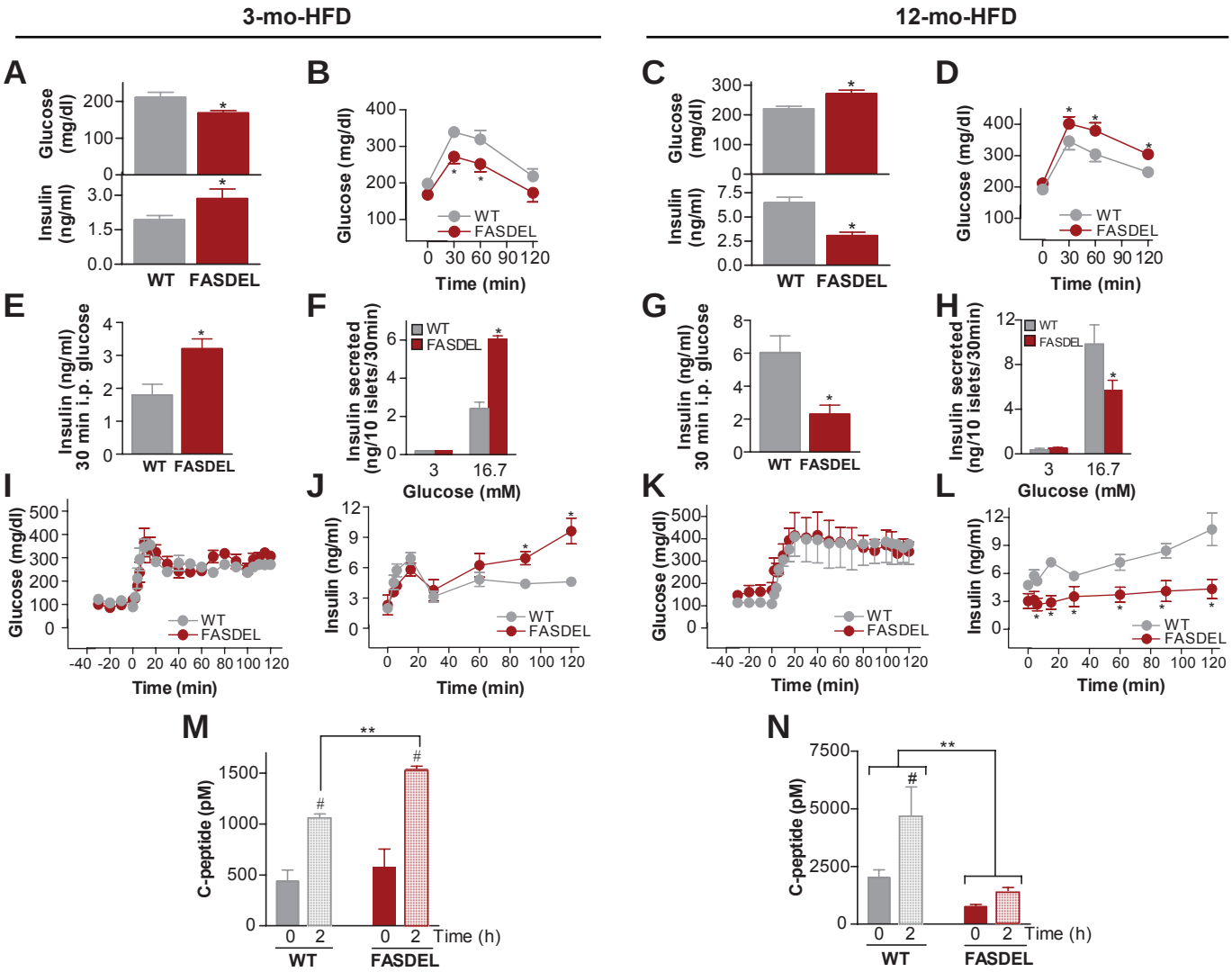

FIG. 3. Glucose homeostasis on HFD at 3 and 12 months of age. *A–D*: Serum glucose (*A* and *C*, *top panels*), serum insulin (*A* and *C*, *bottom panels*), and intraperitoneal glucose tolerance tests (*B* and *D*) at the indicated ages following a 6-h fast. *E–H*: Insulin concentration in the serum 30 min after the glucose load (*E* and *G*) and in the media of cultured islets 30 min after 3 and 16.7 mmol/l glucose (*F* and *H*). *I–N*: Clamped glucose concentration during a 2-h hyperglycemic clamp (*I* and *K*) with the corresponding serum insulin levels at the indicated times (*J* and *L*) and the serum C-peptide concentration at baseline (time 0) and at the end of the clamp (2 h) in mice that were 3 (*M*) and 12 (*N*) months. All results are means ± SE of 7–10 animals per group. **P* < 0.05 vs. the corresponding wild-type (WT) mice. #*P* < 0.05 vs. the corresponding baseline (time 0) value. ***P* < 0.05. *B*, *D*, *I*, *J–L*: ○, wild type (WT); ●, FASDEL. *F* and *H*: □, wild type (WT). ■, FASDEL.

tent than 12-month-old wild-type mice (online appendix Table 1).

FASDEL mice maintained a lower weight on a high-fat diet (HFD) at 3 and 12 months of age (Fig. 2*A–D*). Metabolic parameters for both HFD groups were similar at 3 months of age, but feed efficiency was decreased and Vo_2 increased in FASDEL compared with wild-type mice at 12 months of age (online appendix Table 2).

High-fat feeding had opposite effects on insulin levels in 3-month-old compared with 12-month-old FASDEL mice. Three-month-old FASDEL mice on the HFD had lower glucose, hyperinsulinemia (Fig. 3*A*), and enhanced glucose tolerance (Fig. 3*B*) compared with wild-type mice. Twelve-month-old FASDEL mice on the HFD were hyperglycemic (Fig. 3*C*, *top*), hypoinsulinemic (Fig. 3*C*, *bottom*), and glucose intolerant (Fig. 3*D*), which is striking because adiposity was decreased in FASDEL mice (online appendix Table 2).

FASDEL β-cell function was increased in early life and decreased in later life. In 3-month-old HFD-fed FASDEL mice, insulin levels were higher than in controls after glucose injection (Fig. 3*E*), and cultured islets from these mice secreted 2.5-fold more insulin than controls in response to glucose (Fig. 3*F*). By 12 months the pattern was reversed; insulin secretion was decreased in FASDEL compared with wild-type mice (Fig. 3*G* and *H*). Similar trends were present in 6- and 10-month-old FASDEL mice (not shown).

Insulin secretory function was also studied using a square-wave hyperglycemic clamp. With glucose between 300 and 350 mg/dl for 2 h (Fig. 3*I* and *K*), insulin (Fig. 3*J*) and C-peptide (Fig. 3*M*) secretion were increased in young FASDEL mice and decreased (Fig. 3*L* and *N*) in old FASDEL mice compared with wild-type mice. Insulin content of pancreas and islets (online appendix Table 2) mirrored age-dependent effects on insulin secretion. Insulin mRNA content was unaffected (not shown). Thus, FAS haploinsufficiency produces insulin hypersecretion in early life and hyposecretion with age.

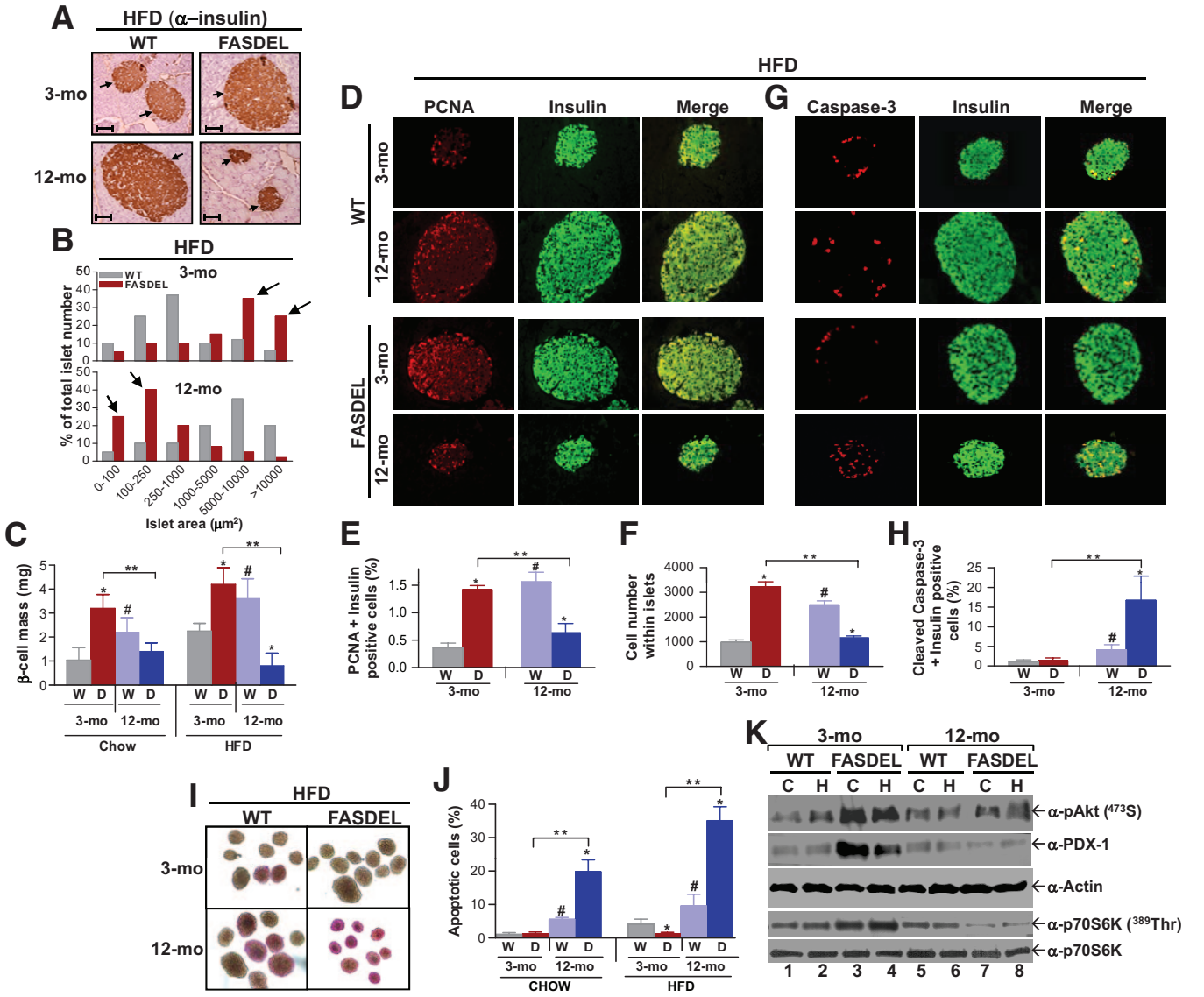

FIG. 4. Failure of β-cell compensation with age and high-fat feeding in FASDEL mice is caused by decreased β-cell proliferation and increased apoptosis. *A*: Representative pancreatic sections immunostained with anti-insulin antibody. The arrows depict insulin-positive areas within each islet surrounded by normal pancreatic acinar cells (×20 magnification). WT, wild type. *B*: Distribution of islet areas after 10 weeks of HFD; arrows highlight the preponderance of larger and smaller islet areas in 3- and 12-month-old FASDEL mice, respectively ($n = 5$). *C*: Changes in β-cell mass on standard chow or HFD at the indicated ages in WT (W) and FASDEL (D) mice ($n = 6$). *D* and *E*: Representative pancreatic sections double immunostained with anti-PCNA (red) and anti-insulin (green) antibodies and visualized using a dual red-green filter at ×20 magnification. Yellow areas in the merged panels represent β-cells expressing PCNA (*D*), which were quantified as a percentage of total insulin positive cells (*E*) ($n = 6$). *D*: WT, wild type; *E*: W, wild type; D, FASDEL. *F*: Number of cells within each islet (from at least 50 islets) counted from 3- and 12-month-old HFD fed mice. W, wild type; D, FASDEL. *G* and *H*: Representative pancreatic sections double immunostained with anti-cleaved caspase-3 (red) and anti-insulin (green) antibodies, visualized using a dual red-green filter at ×20 magnification and quantified as in *E* ($n = 6$). *G*: WT, wild type; *H*: W, wild type; D, FASDEL. *I* and *J*: Representative micrographs (×10 magnification) of dispersed islets stained with the ApoPercentage dye (*I*), which are quantified as a percentage of total islets isolated from both standard chow– and HFD-fed wild-type and FASDEL mice at the indicated ages (*J*) ($n = 5$). *I*: WT, wild type; *J*: W, wild type; D, FASDEL. Representative immunoblots of islets (100 islets per lane) isolated from mice fed standard chow (C) and HFD (H) using the indicated antibodies. WT, wild type. All results are means ± SE. *$P < 0.05$ vs. the corresponding wild-type mice. #$P < 0.05$ vs. corresponding 3-month-old wild-type mice. **$P < 0.05$. (Please see http://dx.doi.org/10.2337/db08-0404 for a high-quality digital representation of this image.)

β-Cell mass in FASDEL mice. Islet area and β-cell mass in mice on the HFD were increased in 3-month-old FASDEL mice but decreased in 12-month-old wild-type mice (Fig. 4*A*–*C*). Pancreatic weights did not differ by genotype (online appendix Table 2). The same effects on mass were seen with the standard chow diet (Fig. 4*C*) and at 2 and 4 weeks of postnatal life (not shown). Unlike wild-type mice, which compensated for age and high-fat feeding by increasing β-cell mass (Fig. 4*C*), 12-month-old FASDEL mice had and approximately fourfold-reduced β-cell mass (Fig. 4*C*). This was not due to FAS deficiency, since β-cell–specific FAS knockout mice have no β-cell phenotype (21).

β-Cell mass, a predictor of diabetes (9), reflects cell proliferation, size, neogenesis, and apoptosis (30). Proliferation, assessed in vivo with PCNA staining, was increased in 3-month-old FASDEL compared with wild-type islets with the HFD (Fig. 4*D* and *E*). Wild-type mice demonstrated an approximately fourfold compensatory increase with age in the number of proliferating β-cells, but older FASDEL mice had a 39% decrease (Fig. 4*E*). Similar results were seen with standard chow (not

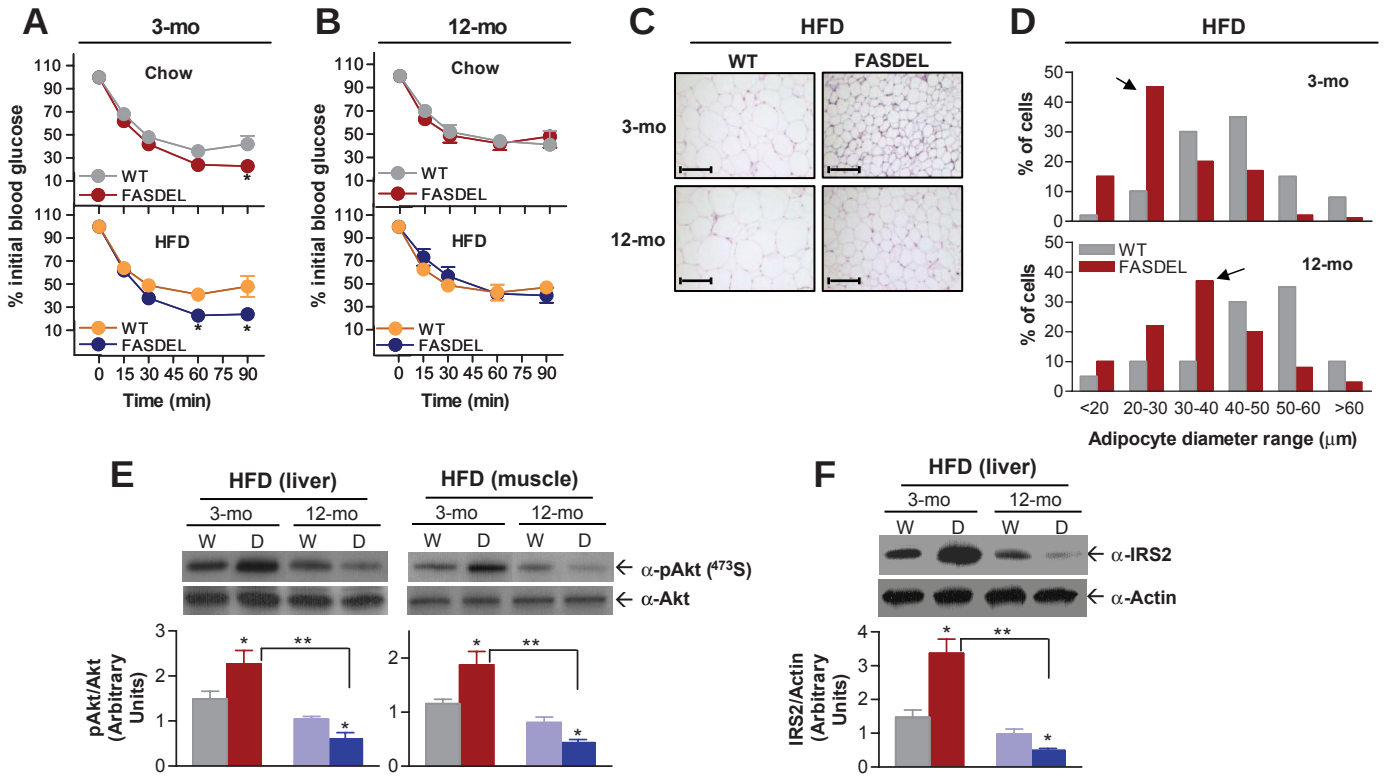

FIG. 5. FASDEL mice are not insulin resistant. *A* and *B*: Insulin tolerance tests. Blood glucose concentration before and after intraperitoneal injection of insulin in standard chow– and HFD-fed mice ($n = 6$). △ and ○, wild type (WT); ▲ and ●, FASDEL. *C*: Representative hematoxylin and eosin–stained histologic sections (× 20 magnification) of white adipose tissue from gonadal fat pads of 3- and 12-month-old male mice after 10 weeks of HFD feeding. WT, wild type. *D*: The distribution curve of diameter of 300 fat cells per mouse shows a preponderance of small-sized (20- to 40-μm) adipocytes (arrows) in the FASDEL mice compared with controls ($n = 5$). □, wild type (WT); ■, FASDEL. *E* and *F*: Western blotting for phosphorylated and total Akt and total IRS-2 proteins in liver and skeletal muscles obtained from wild-type (W) and FASDEL (D) mice (*top panel*) in the fed state and the densitometric analysis of such blots from four mice per group (*bottom panel*). Data represent means ± SE. *$P < 0.05$ vs. the corresponding wild-type mice. **$P < 0.05$. (Please see http://dx.doi.org/10.2337/db08-0404 for a high-quality digital representation of this image.)

shown). Wild-type and FASDEL islets showed similar abundance and staining pattern for α-cells as well as for acinar architecture and cell density (not shown).

Islet number was similar in each genotype and age-group on both diets. For example, on the HFD at 12 months, islet number per mm^2 pancreas was 0.84 ± 0.23 in wild-type vs. 0.79 ± 0.43 in FASDEL mice ($n = 6$, P = NS). Dividing β-cell area by β-cell nuclei showed that β-cell size was unaffected by genotype (HFD-fed wild-type mice: 125 ± 4 μm^2, $n = 100$; HFD-fed FASDEL mice: 119 ± 5 μm^2, $n = 110$; P = NS). Similar results were obtained at older ages, on the standard chow diet, and with estimates of cell density (not shown). Three-month-old FASDEL islets had more cells per islet (Fig. 4*F*) and increased DNA content per islet (FASDEL: 42.3 ± 2.3 ng/islet, $n = 8$; wild type: 28.9 ± 1.5 ng/islet, $n = 6$; $P < 0.001$). In the older FASDEL mice, both cell number (Fig. 4*F*) and DNA content per islet (wild type: 54.3 ± 4.3 ng/islet, $n = 8$; FASDEL: 32.9 ± 2.1 ng/islet, $n = 8$; $P < 0.001$) were decreased. Thus, increased β-cell mass in young FAS haploinsufficient mice is due to hyperplasia.

Apoptosis was increased in old, but not young, FASDEL islets. Proapoptotic caspase-3 was unaffected in 3-month-old wild-type and FASDEL islets but increased more than fourfold in FASDEL compared with wild-type islets at 12 months (Fig. 4*G* and *H*). Staining dispersed islets for phosphatidylserine translocation (31) confirmed a >3.5-fold increase in apoptotic cells in 12-month-old FASDEL mice (Fig. 4*I* and *J*).

Phosphorylated Akt and pancreatic duodenal homeobox factor-1, which regulate β-cell mass, islet development, and insulin secretion, were increased in 3-month-old compared with 12-month-old FASDEL islets (Fig. 4*K*, *lanes 3* and *4* vs. *7* and *8*). Total Akt (not shown) and actin content (Fig. 4*K*) were unaffected. Relative to wild-type mice, FASDEL ^{389}Thr phosphorylation of p70S6K was increased at 3 months and decreased at 12 months (Fig. 4*K*, *lanes 3* and *4* vs. *7* and *8*), consistent with growth promotion and apoptosis suppression by this protein.

Insulin responses in FASDEL mice. FASDEL mice were more insulin sensitive than their control littermates at 2 weeks of age (not shown) and at 3 months on both standard chow and HFD (Fig. 5*A*). This effect was not detected at 12 months (Fig. 5*B*). Adipocyte size, reciprocally related to insulin sensitivity, was decreased in HFD-fed FASDEL mice (Fig. 5*C* and *D*) and on standard chow diet (not shown), suggesting that FASDEL mice are not insulin resistant. Phosphorylated Akt in liver and muscle (Fig. 5*E*) and IRS-2 protein (Fig. 5*F*) in liver were increased in young FASDEL compared with wild-type mice. These molecules were decreased in 12-month-old FASDEL mice (Fig. 5*E* and *F*), reflecting their hypoinsulinemia.

Body size and pancreatic β-cell mass. In >15 litters at E18.5 (when distinct islets appear) (31), FAS haploinsufficiency decreased fetal body weight by 21% (Fig. 6*A* and *B*) and body length by 23% compared with wild-type littermates, changes associated with a doubling of β-cell mass (Fig. 6*C* and *D*) (online appendix Fig. 1*A*). Islet area was increased approximately twofold, which is associated

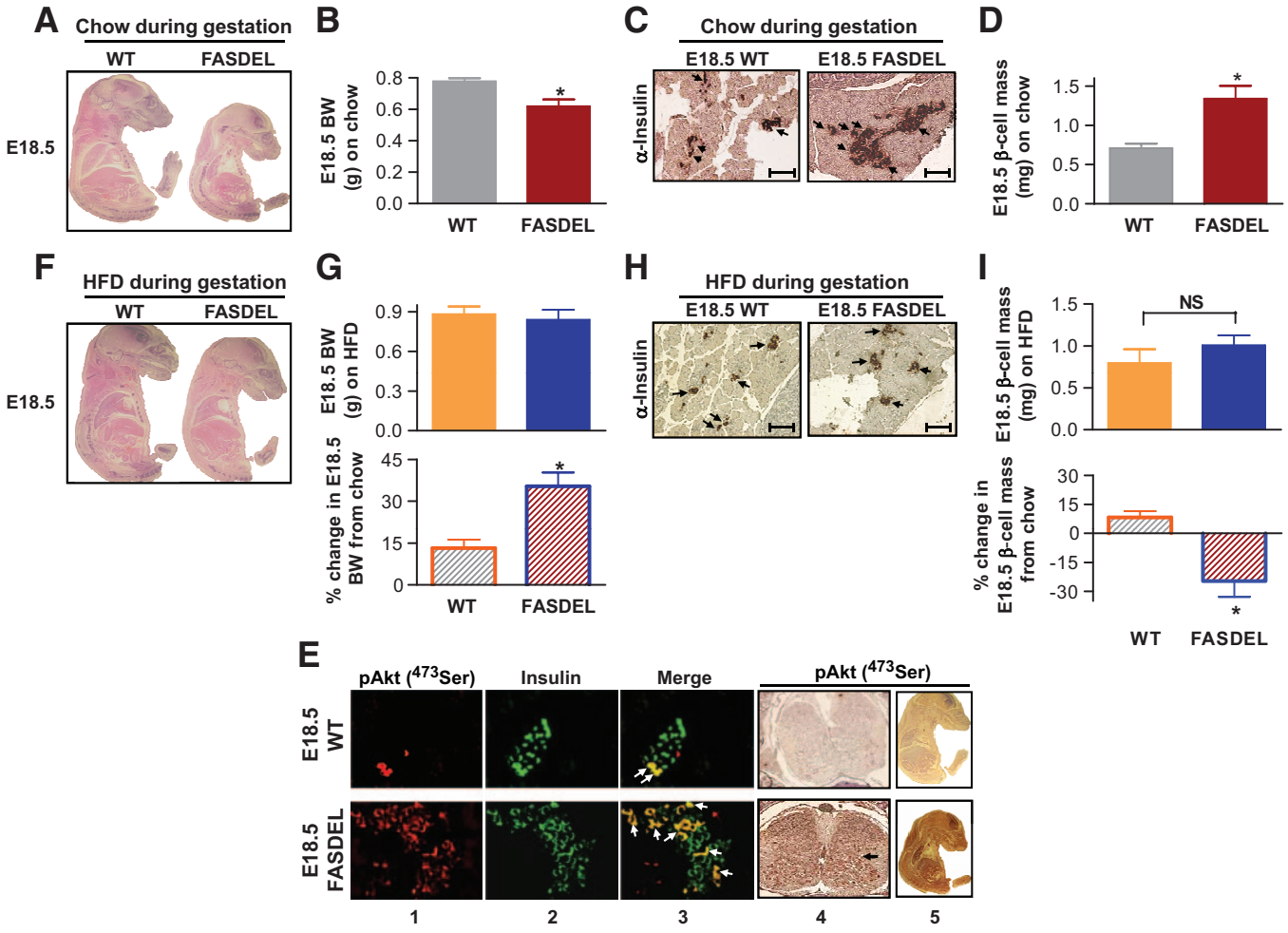

FIG. 6. β-Cells respond to intrauterine body size. *A* and *B*: Representative whole-mount sections of E18.5 fetuses from standard chow–fed dams stained with hematoxylin and eosin (*A*) and fetal body weights (*B*) (n = 12). WT, wild type. *C*: Representative pancreatic sections immunostained with anti-insulin antibody. The arrows depict insulin-positive areas within each islet surrounded by normal pancreatic acinar cells (×10 magnification). WT, wild type. *D*: β-Cell mass in E18.5 fetuses (n = 12). WT, wild type. *E*: Representative pancreatic sections double immunostained with antiphosphorylated Akt (red, *panel 1*) and anti-insulin (green, *panel 2*) and visualized using a dual red-green filter (merged, *panel 3*) at ×20 magnification. Arrows in *panel 3* identify β-cells expressing phosphorylated Akt (yellow). Representative sections of cerebral hemispheres from E18.5 fetuses (*panel 4*) and whole-mount sections (*panel 5*) stained with phosphorylated Akt (brown staining). Arrow in *panel 4* indicates phosphorylated Akt–positive areas. WT, wild type. *F*: Representative whole-mount sections of E18.5 fetuses from HFD-fed dams (HFD fed from day 0.5 to day 18.5) stained with hematoxylin and eosin. WT, wild type. *G*: Weights of fetuses from HFD-fed dams (*top panel*) and the percentage change in body weight compared with fetuses from standard chow–fed dams (*bottom panel*) (n = 10). WT, wild type. *H*: Representative pancreatic sections (×10 magnification) immunostained with anti-insulin antibody as in *C*. WT, wild type. *I*: β-Cell mass in E18.5 fetuses from HFD-fed dams (*top panel*) and the percentage change in β-cell mass compared with fetuses from standard chow–fed dams (*bottom panel*) (n = 10). WT, wild type. Results are means ± SE. *P < 0.05 vs. the corresponding wild type mice. (Please see http://dx.doi.org/10.2337/db08-0404 for a high-quality digital representation of this image.)

with increased proliferation and decreased apoptosis (Table 1) without effect on β-cell size or density (not shown). Since pancreatic weight, acinar architecture, and α-cells were unaffected (not shown), increased E18.5 FASDEL insulin content (Table 1) appears to be due to increased β-cell mass. Increased phosphorylated Akt was present in E18.5 islets and whole fetus (especially brain) (Fig. 6*E*), suggesting that expanded β-cell mass in FASDEL fetuses is

TABLE 1
Morphometric parameters in E18.5 wild-type and FASDEL fetuses after feeding either standard chow or HFD to dams during gestation

	Standard chow during gestation		HFD during gestation	
Parameters at E18.5	Wild type	FASDEL	Wild type	FASDEL
Islet number per mm^2	0.28 ± 0.06	0.31 ± 0.09	0.29 ± 0.12	0.32 ± 0.14
Islet area (%)	0.54 ± 0.09	1.04 ± 0.07*	0.58 ± 0.10	0.80 ± 0.07†
Insulin plus PCNA-positive cells (%)	1.02 ± 0.22	2.14 ± 0.14*	1.34 ± 0.17	1.67 ± 0.11†
Insulin plus caspase-3–positive cells (%)	4.70 ± 1.10	1.12 ± 0.18*	4.50 ± 1.80	2.28 ± 0.14*†
Insulin content (ng/mg pancreas)	50.1 ± 5.7	73.4 ± 3.2*	54.7 ± 3.8	62.8 ± 3.5†

Data are means ± SE. Complete pancreas sections from 10 to 12 fetuses at E18.5 of each genotype were analyzed. *P < 0.05 vs. the corresponding wild-type control. †P < 0.05 vs. the FASDEL fetuses from standard chow–fed dams during gestation.

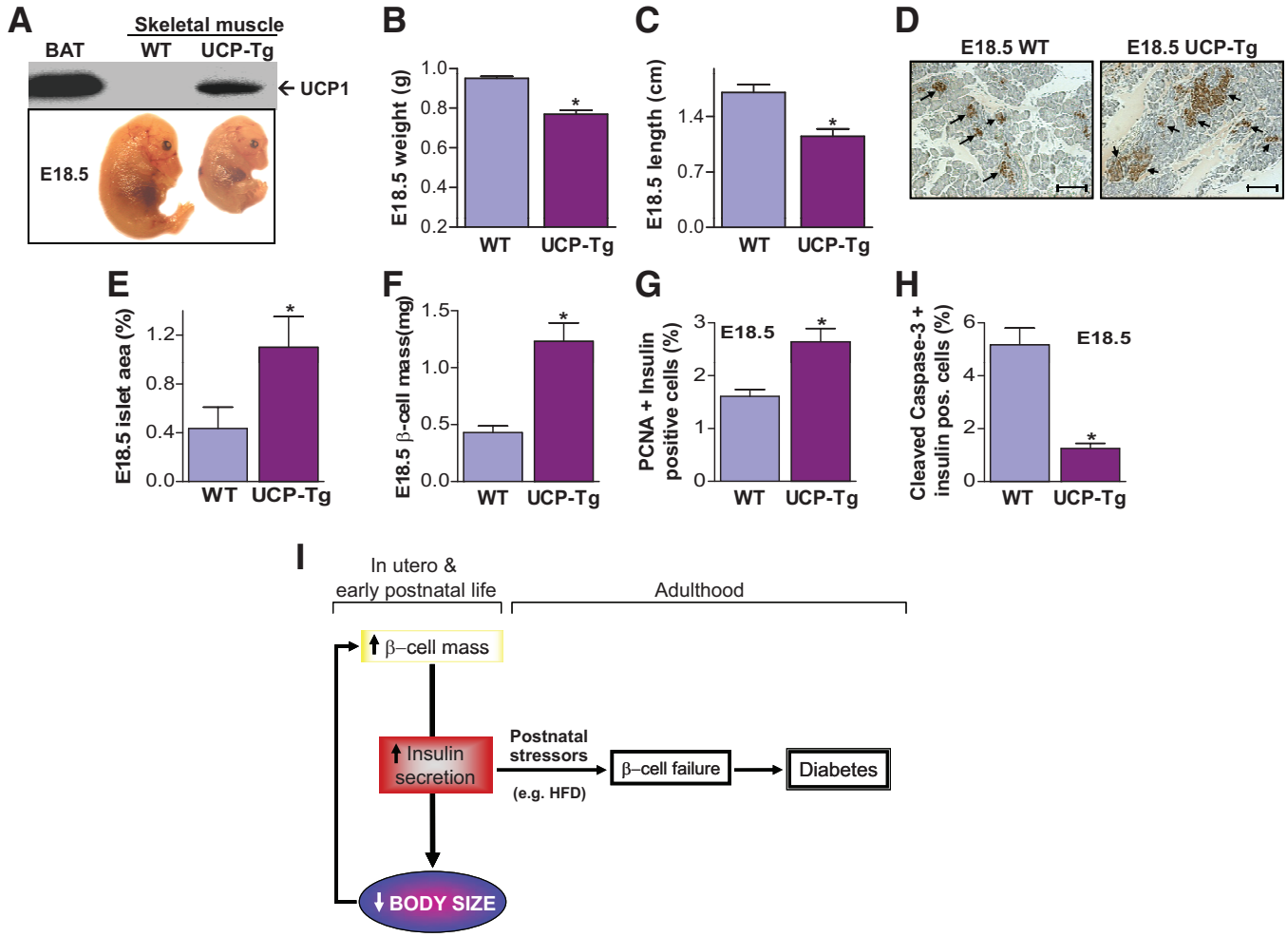

FIG. 7. Increased fetal β-cell mass in an FAS-independent model of intrauterine growth restriction. *A*: Transgenic overexpression of UCP-1 in skeletal muscle (UCP-Tg), confirmed by Western blotting using UCP-1 antibody (*top panel*), leads to intrauterine growth restriction at E18.5 (*bottom panel*). BAT, brown adipose tissue. WT, wild type. *B* and *C*: UCP-Tg fetuses have decreased body weight (*B*) and length (*C*). WT, wild type. *D*: Representative pancreatic sections immunostained with anti-insulin antibody. The arrows depict insulin-positive areas within each islet surrounded by normal pancreatic acinar cells (× 10 magnification). WT, wild type. *E* and *F*: Islet area (*E*) and total β-cell mass (*F*). WT, wild type. *G* and *H*: Replication of β-cells assayed by PCNA and insulin double immunostaining (*G*) and apoptosis assayed by cleaved caspase-3 and insulin double immunostaining (*H*) from pancreatic sections of E18.5 wild-type (WT) and UCP-Tg fetuses. All results are means ± SE of 10–12 mice per group. *$P < 0.05$ compared vs. the corresponding wild-type mice. *I*: Model for the developmental programming of pancreatic β-cells. β-Cells respond to intrauterine body size by modulating insulin secretion. Early hypersecretion of insulin likely represents an adaptation to allow optimal fetal growth. However, this early increase entrains β-cell failure with age leading to diabetes. (Please see http://dx.doi.org/10.2337/db08-0404 for a high-quality digital representation of this image.)

not due to insulin resistance. In support of this notion, glucose and free fatty acid levels were decreased, whereas insulin levels were increased in E18.5 fetuses (online appendix Table 3).

Feeding a HFD instead of standard chow to timed-pregnant females to force fetal growth preferentially increased the size of FASDEL mice and abolished the genotype difference in body weight (Fig. 6*F* and *G*) and β-cell mass (Fig. 6*H* and *I*). E18.5 FASDEL fetuses from HFD-fed dams with increased body size showed a 25% reduction in β-cell mass (Fig. 6*G* and *I*, *bottom*) (online appendix Fig. 1*A*) and a 23% decrease in islet area (Table 1), largely due to an increase in apoptosis compared with FASDEL fetuses from standard chow–fed dams (Table 1).

The association between fetal body size and fetal β-cell mass was also confirmed in a different model of intrauterine growth restriction, mice with ectopic expression of UCP-1 in skeletal muscle (25,26) (Fig. 7*A*, *top*). Decreased body size (Fig. 7*A–C*) persists and peripheral insulin sensitivity is increased in these mice (26). Islet area and β-cell mass in E18.5 UCP-1 fetuses from >10 litters were inversely associated with intrauterine body size (Fig. 7*D–F*) (online appendix Fig. 1*B*). Increased β-cell mass was due to a combination of increased β-cell proliferation and decreased apoptosis (Fig. 7*G* and *H*).

DISCUSSION

Small infants have abnormal glucose metabolism as adults, often preceded by the complicating effects of catch-up growth (32,33). Here, we demonstrate that IUGR, in the absence of insulin resistance or catch-up growth, is associated with pancreatic β-cell hyperplasia with hyperfunction in early life and β-cell loss with secretory failure in later life. These findings identify β-cell–specific developmental programming as a potential contributor to insulin secretory dysfunction and disease.

In utero growth restriction was associated with an expansion of β-cell mass (Figs. 4*A* and 6*C*). Glucose and insulin are unlikely to be responsible. Glucose can stimulate β-cell replication (34), but islet hyperplasia occurs without hyperglycemia (35). Hyperinsulinemia and insulin

signaling have been implicated in expansion of β-cell mass (36,37), but mice lacking insulin genes (*Ins1*$^{-/-}$*Ins2*$^{-/-}$) (12,38) and both the insulin receptor and *Igf1* receptor (*Insr*$^{-/-}$*Igf1r*$^{-/-}$) (39) have increased fetal β-cell mass, which is the opposite of expected results if β-cell growth were insulin dependent. Though we cannot rule out effects of FAS deficiency in other tissues on β-cell mass, a specific decrease in β-cell FAS expression is unlikely to contribute to the phenotype in FASDEL mice since β-cell–specific inactivation of FAS has no effect on β-cell mass or function (21).

Instead, the data suggest that intrauterine body size may regulate β-cell mass. Both FASDEL and UCP-Tg E18.5 fetuses, distinct models with in utero growth restriction (Figs. 6*A* and 7*A*) achieved through different mechanisms, had increased β-cell mass (Figs. 6*D* and 7*F*) (online appendix Fig. 1). Growth-restricted double knockout *Ins1*$^{-/-}$*Ins2*$^{-/-}$ and *Insr*$^{-/-}$*Igf1r*$^{-/-}$mice (12,39) also have increased fetal β-cell mass. Single knockout *Insr*$^{-/-}$ mice are not growth restricted and have normal fetal β-cell mass (40).

However, not all models show a clear link between body size and β-cells. Decreased fetal body size induced by maternal protein restriction in the last trimester of pregnancy in rats increased β-cell insulin content in E21.5 fetuses, but their β-cell mass was reduced (41). The Goto-Kakisaki rat, a type 2 diabetes model, has decreased β-cell mass in E21.5 fetuses, but E21.5 body weights of Goto-Kakisaki and wild-type animals are similar (42). In addition, offspring from other IUGR models, achieved by maternal caloric restriction (5) or by ligating the uterine arteries (8), either show no alteration in β-cell mass or have decreased islet mass with IUGR, respectively. These models, in contrast to the FASDEL mice, produce catch-up growth and glucose intolerance.

The hypothesis of β-cell mass regulation by body size is supported by our data, showing that overcoming IUGR with high-fat feeding of dams during gestation normalized both fetal β-cell mass (Fig. 6*H* and *I*) and pancreatic insulin content (Table 1) in E18.5 FASDEL fetuses. These data also demonstrate nutrition-dependent developmental plasticity, as high-fat feeding does not correct the FASDEL phenotype in adulthood. This implies the existence of a critical time period in utero allowing modification of fetal growth to impact β-cell function. β-Cell adaptation to body size is plastic during development, and this plasticity establishes a template for metabolic homeostasis in adulthood.

Insulin signaling, while not critical for fetal β-cell growth, does appear to be responsible for the growth of most other somatic tissues in utero. In *Drosophila*, inactivation of insulin production (15), the insulin receptor (11), and several downstream signaling components, including IRSs (10), phosphoinositide 3-kinase (13), and p70S6 kinase (14), decreases body size. Double knockout *Ins1*$^{-/-}$*Ins2*$^{-/-}$ and double knockout *Insr*$^{-/-}$*Igf1r*$^{-/-}$ mice (12,39) are growth retarded as are mice with inactivation of IRS-1 (43). Consistent with these observations, increased β-cell mass in both FASDEL (Figs. 4*A* and 6*C*) and UCP-Tg (Fig. 7*D*) mice likely represents a homeostatic response to normalize intrauterine growth. This concept is presented schematically in Fig. 7*I*. Decreased body size could prompt an increase in β-cell mass, leading to increased insulin secretion in an attempt to normalize body size by promoting growth. A similar adaptive response may be seen in small-for-gestational-age humans, who manifest insulin levels 2.5-fold higher than controls (44), mirroring hyperinsulinemia in young FASDEL mice (Fig. 3*A*, *bottom*). These data, in concert with our demonstration that increasing intrauterine growth (Fig. 6*F* and *G*) normalized fetal β-cell mass (Fig. 6*H* and *I*), imply that optimal body size might be sensed and provide feedback to pancreatic β-cells (Fig. 7*I*), the only cell type that produces insulin. β-Cells respond to nutrients and other signals during development (17,31), making them ideal for integrating inputs to coordinate growth. A precedent for sensing optimal body size involving insulin signaling exists in *Drosophila* (16).

Data for β-cell mass in humans with IUGR are inconsistent. One group reported a decrease (45) and another no change in islets from IUGR fetuses (46). These data are not directly comparable with our work because we studied mice near the end of gestation (E18.5), while human fetuses in both of these studies were analyzed early in the third trimester when islet morphogenesis is not complete.

Our results suggest that β-cell hyperfunction, even when it occurs in the absence of peripheral insulin resistance, can lead to insulin secretory failure. Increased β-cell mass and insulin hypersecretion in early life (Fig. 3) entrains β-cells to fail in later life (Figs. 3, 4, and 7*I*). These data provide a mechanistic basis for observations made in Pima Indians, people with an unusually high prevalence of diabetes despite hyperinsulinemia and intact insulin sensitivity (47). Among Nauruans, progression to diabetes is associated with loss of insulin secretory capacity rather than a loss of insulin sensitivity (48), a phenomenon recapitulated in FASDEL mice. Our data are also consistent with previous work (49) associating early increases in β-cell mass with defects in insulin secretion undermining β-cell compensation required to maintain glucose homeostasis with age. The underlying reason is unclear, but an inadequate blood supply in hyperplastic islets could be involved (50).

A perhaps surprising outcome of recent genome-wide association studies was the observation that β-cell genes are the dominant driver of metabolic disease. Our work indicates that intrauterine body size appears to be sensed and integrated through the β-cell to modulate insulin secretion. Increased β-cell mass developing in response to decreased body size programs the β-cell to fail, possibly by limiting its capacity to adapt to conditions, such as high-fat feeding, that demand increased insulin secretion. FASDEL mice could be useful for defining the mechanisms underlying β-cell failure.

ACKNOWLEDGMENTS

This work was funded by the American Diabetes Association (Junior Faculty Award 1-07-JF-12 to M.V.C. and a Mentor-Based Postdoctoral Fellowship Award), National Institutes of Health Grants DK076729 and P50 HL083762, and the Clinical Nutrition Research Unit (DK56341) and Diabetes Research and Training Center (DK20579).

We thank Sonia Najjar for providing anti-FAS antibodies.

REFERENCES

1. Gluckman PD, Hanson MA: Living with the past: evolution, development, and patterns of disease. *Science* 305:1733–1736, 2004
2. Kajantie E, Osmond C, Barker DJ, Forsen T, Phillips DI, Eriksson JG: Size at birth as a predictor of mortality in adulthood: a follow-up of 350 000 person-years. *Int J Epidemiol* 34:655–663, 2005
3. Barker DJ, Osmond C: Infant mortality, childhood nutrition, and ischaemic heart disease in England and Wales. *Lancet* 1:1077–1081, 1986

4. Barker DJ, Osmond C, Forsen TJ, Kajantie E, Eriksson JG: Trajectories of growth among children who have coronary events as adults. *N Engl J Med* 353:1802–1809, 2005
5. Jimenez-Chillaron JC, Hernandez-Valencia M, Reamer C, Fisher S, Joszi A, Hirshman M, Oge A, Walrond S, Przybyla R, Boozer C, Goodyear LJ, Patti ME: β-Cell secretory dysfunction in the pathogenesis of low birth weight-associated diabetes: a murine model. *Diabetes* 54:702–711, 2005
6. Bertin E, Gangnerau MN, Bailbe D, Portha B: Glucose metabolism and beta-cell mass in adult offspring of rats protein and/or energy restricted during the last week of pregnancy. *Am J Physiol* 277:E11–E17, 1999
7. Nyirenda MJ, Lindsay RS, Kenyon CJ, Burchell A, Seckl JR: Glucocorticoid exposure in late gestation permanently programs rat hepatic phosphoenolpyruvate carboxykinase and glucocorticoid receptor expression and causes glucose intolerance in adult offspring. *J Clin Invest* 101:2174–2181, 1998
8. Simmons RA, Templeton LJ, Gertz SJ: Intrauterine growth retardation leads to the development of type 2 diabetes in the rat. *Diabetes* 50:2279–2286, 2001
9. Prentki M, Nolan CJ: Islet beta cell failure in type 2 diabetes. *J Clin Invest* 116:1802–1812, 2006
10. Bohni R, Riesgo-Escovar J, Oldham S, Brogiolo W, Stocker H, Andruss BF, Beckingham K, Hafen E: Autonomous control of cell and organ size by CHICO, a Drosophila homolog of vertebrate IRS1–4. *Cell* 97:865–875, 1999
11. Chen C, Jack J, Garofalo RS: The Drosophila insulin receptor is required for normal growth. *Endocrinology* 137:846–856, 1996
12. Duvillie B, Cordonnier N, Deltour L, Dandoy-Dron F, Itier JM, Monthioux E, Jami J, Joshi RL, Bucchini D: Phenotypic alterations in insulin-deficient mutant mice. *Proc Natl Acad Sci U S A* 94:5137–5140, 1997
13. Leevers SJ, Weinkove D, MacDougall LK, Hafen E, Waterfield MD: The Drosophila phosphoinositide 3-kinase Dp110 promotes cell growth. *EMBO J* 15:6584–6594, 1996
14. Montagne J, Stewart MJ, Stocker H, Hafen E, Kozma SC, Thomas G: Drosophila S6 kinase: a regulator of cell size. *Science* 285:2126–2129, 1999
15. Rulifson EJ, Kim SK, Nusse R: Ablation of insulin-producing neurons in flies: growth and diabetic phenotypes. *Science* 296:1118–1120, 2002
16. Colombani J, Bianchini L, Layalle S, Pondeville E, Dauphin-Villemant C, Antoniewski C, Carre C, Noselli S, Leopold P: Antagonistic actions of ecdysone and insulins determine final size in Drosophila. *Science* 310:667–670, 2005
17. Ackermann AM, Gannon M: Molecular regulation of pancreatic beta-cell mass development, maintenance, and expansion. *J Mol Endocrinol* 38:193–206, 2007
18. Semenkovich CF: Regulation of fatty acid synthase (FAS). *Prog Lipid Res* 36:43–53, 1997
19. Chirala SS, Chang H, Matzuk M, Abu-Elheiga L, Mao J, Mahon K, Finegold M, Wakil SJ: Fatty acid synthesis is essential in embryonic development: fatty acid synthase null mutants and most of the heterozygotes die in utero. *Proc Natl Acad Sci U S A* 100:6358–6363, 2003
20. Chakravarthy MV, Pan Z, Zhu Y, Tordjman K, Schneider JG, Coleman T, Turk J, Semenkovich CF: "New" hepatic fat activates PPARalpha to maintain glucose, lipid, and cholesterol homeostasis. *Cell Metab* 1:309–322, 2005
21. Chakravarthy MV, Zhu Y, Lopez M, Yin L, Wozniak DF, Coleman T, Hu Z, Wolfgang M, Vidal-Puig A, Lane MD, Semenkovich CF: Brain fatty acid synthase activates PPARalpha to maintain energy homeostasis. *J Clin Invest* 117:2539–2552, 2007
22. Terauchi Y, Kubota N, Tamemoto H, Sakura H, Nagai R, Akanuma Y, Kimura S, Kadowaki T: Insulin effect during embryogenesis determines fetal growth: a possible molecular link between birth weight and susceptibility to type 2 diabetes. *Diabetes* 49:82–86, 2000
23. Withers DJ, Gutierrez JS, Towery H, Burks DJ, Ren JM, Previs S, Zhang Y, Bernal D, Pons S, Shulman GI, Bonner-Weir S, White MF: Disruption of IRS-2 causes type 2 diabetes in mice. *Nature* 391:900–904, 1998
24. Lakso M, Pichel JG, Gorman JR, Sauer B, Okamoto Y, Lee E, Alt FW, Westphal H: Efficient in vivo manipulation of mouse genomic sequences at the zygote stage. *Proc Natl Acad Sci U S A* 93:5860–5865, 1996
25. Li B, Nolte LA, Ju JS, Han DH, Coleman T, Holloszy JO, Semenkovich CF: Skeletal muscle respiratory uncoupling prevents diet-induced obesity and insulin resistance in mice. *Nat Med* 6:1115–1120, 2000
26. Han DH, Nolte LA, Ju JS, Coleman T, Holloszy JO, Semenkovich CF: UCP-mediated energy depletion in skeletal muscle increases glucose transport despite lipid accumulation and mitochondrial dysfunction. *Am J Physiol Endocrinol Metab* 286:E347–E353, 2004
27. Bernal-Mizrachi E, Wen W, Stahlhut S, Welling CM, Permutt MA: Islet beta cell expression of constitutively active Akt1/PKB alpha induces striking hypertrophy, hyperplasia, and hyperinsulinemia. *J Clin Invest* 108:1631–1638, 2001
28. DeFronzo RA, Tobin JD, Andres R: Glucose clamp technique: a method for quantifying insulin secretion and resistance. *Am J Physiol* 237:E214–E223, 1979
29. Johnson JD, Ahmed NT, Luciani DS, Han Z, Tran H, Fujita J, Misler S, Edlund H, Polonsky KS: Increased islet apoptosis in $Pdx1^{+/-}$ mice. *J Clin Invest* 111:1147–1160, 2003
30. Bonner-Weir S: Life and death of the pancreatic beta cells. *Trends Endocrinol Metab* 11:375–378, 2000
31. Kim SK, Hebrok M: Intercellular signals regulating pancreas development and function. *Genes Dev* 15:111–127, 2001
32. Hales CN, Barker DJ, Clark PM, Cox LJ, Fall C, Osmond C, Winter PD: Fetal and infant growth and impaired glucose tolerance at age 64. *BMJ* 303:1019–1022, 1991
33. Hovi P, Andersson S, Eriksson JG, Jarvenpaa AL, Strang-Karlsson S, Makitie O, Kajantie E: Glucose regulation in young adults with very low birth weight. *N Engl J Med* 356:2053–2063, 2007
34. Weir GC, Bonner-Weir S: A dominant role for glucose in beta cell compensation of insulin resistance. *J Clin Invest* 117:81–83, 2007
35. Bruning JC, Winnay J, Bonner-Weir S, Taylor SI, Accili D, Kahn CR: Development of a novel polygenic model of NIDDM in mice heterozygous for IR and IRS-1 null alleles. *Cell* 88:561–572, 1997
36. Okamoto H, Hribal ML, Lin HV, Bennett WR, Ward A, Accili D: Role of the forkhead protein FoxO1 in beta cell compensation to insulin resistance. *J Clin Invest* 116:775–782, 2006
37. Okada T, Liew CW, Hu J, Hinault C, Michael MD, Krtzfeldt J, Yin C, Holzenberger M, Stoffel M, Kulkarni RN: Insulin receptors in beta-cells are critical for islet compensatory growth response to insulin resistance. *Proc Natl Acad Sci U S A* 104:8977–8982, 2007
38. Duvillie B, Currie C, Chrones T, Bucchini D, Jami J, Joshi RL, Hill DJ: Increased islet cell proliferation, decreased apoptosis, and greater vascularization leading to beta-cell hyperplasia in mutant mice lacking insulin. *Endocrinology* 143:1530–1537, 2002
39. Kido Y, Nakae J, Hribal ML, Xuan S, Efstratiadis A, Accili D: Effects of mutations in the insulin-like growth factor signaling system on embryonic pancreas development and beta-cell compensation to insulin resistance. *J Biol Chem* 277:36740–36747, 2002
40. Accili D, Drago J, Lee EJ, Johnson MD, Cool MH, Salvatore P, Asico LD, Jose PA, Taylor SI, Westphal H: Early neonatal death in mice homozygous for a null allele of the insulin receptor gene. *Nat Genet* 12:106–109, 1996
41. Bertin E, Gangnerau MN, Bellon G, Bailbé D, Arbelot De Vacqueur A, Portha B: Development of beta-cell mass in fetuses of rats deprived of protein and/or energy in last trimester of pregnancy. *Am J Physiol Regul Integr Comp Physiol* 283:R623–R630, 2002
42. Serradas P, Gangnerau MN, Giroix MH, Saulnier C, Portha B: Impaired pancreatic beta cell function in the fetal GK rat: impact of diabetic inheritance. *J Clin Invest* 101:899–904, 1998
43. Tamemoto H, Kadowaki T, Tobe K, Yagi T, Sakura H, Hayakawa T, Terauchi Y, Ueki K, Kaburagi Y, Satoh S, Sekihara H, Yoshioka S, Horikoshi H, Furuta Y, Ikawa Y, Kasuga M, Yazaki Y, Aizawa S: Insulin resistance and growth retardation in mice lacking insulin receptor substrate-1. *Nature* 372:182–186, 1994
44. Wang X, Cui Y, Tong X, Ye H, Li S: Glucose and lipid metabolism in small-for-gestational-age infants at 72 hours of age. *J Clin Endocrinol Metab* 92:681–684, 2007
45. Van Assche FA, De Prins F, Aerts L, Verjans M: The endocrine pancreas in small-for-dates infants. *Br J Obstet Gynaecol* 84:751–753, 1977
46. Beringue F, Blondeau B, Castellotti MC, Breant B, Czernichow P, Polak M: Endocrine pancreas development in growth-retarded human fetuses. *Diabetes* 51:385–391, 2002
47. Weyer C, Hanson RL, Tataranni PA, Bogardus C, Pratley RE: A high fasting plasma insulin concentration predicts type 2 diabetes independent of insulin resistance: evidence for a pathogenic role of relative hyperinsulinemia. *Diabetes* 49:2094–2101, 2000
48. Sicree RA, Zimmet PZ, King HO, Coventry JS: Plasma insulin response among Nauruans: prediction of deterioration in glucose tolerance over 6 years. *Diabetes* 36:179–186, 1987
49. Laybutt DR, Weir GC, Kaneto H, Lebet J, Palmiter RD, Sharma A, Bonner-Weir S: Overexpression of c-Myc in β-cells of transgenic mice causes proliferation and apoptosis, downregulation of insulin gene expression, and diabetes. *Diabetes* 51:1793–1804, 2002
50. Li X, Zhang L, Meshinchi S, Dias-Leme C, Raffin D, Johnson JD, Treutelaar MK, Burant CF: Islet microvasculature in islet hyperplasia and failure in a model of type 2 diabetes. *Diabetes* 55:2965–2973, 2006